CHAM

CFD Modelling of a Micro Shock Tube
Dr Michael Malin / Mr Jason Cooke
January 2016 (amended Jan 2018)

Introduction

Traditional macro shock tubes have a long history in aerodynamics but, more recently, micro shock tubes have been used extensively in many engineering applications, such as micro-propulsion systems and drug-delivery devices for medical systems. A shock tube has closed ends, and the flow is generated by the rupture of a diaphragm separating a driver gas at high pressure from a driven gas at low pressure. This rupture results in the movement of a shock wave and contact discontinuity into the low-pressure gas, and an expansion wave into the high pressure gas. The major difference between micro and macro shock tubes is that the small flow dimension introduces additional flow physics. In particular, micro shock tubes experience shock attenuation from significant viscous effects at low Reynolds numbers. In addition, at high Knudsen numbers, there is slipping of the near-wall fluid due to non-continuum effects, and this acts to increase shock strength and aid shock wave propagation. The micro shock tube described below is one of several cases investigated by the Gas Dynamics Laboratory of the Andong National University of South Korea employing a variety of well-known CFD packages for comparison purposes. CHAM was approached to provide guidance in using PHOENICS® to set up and simulate flow in the micro shock tube shown in Figure 1.

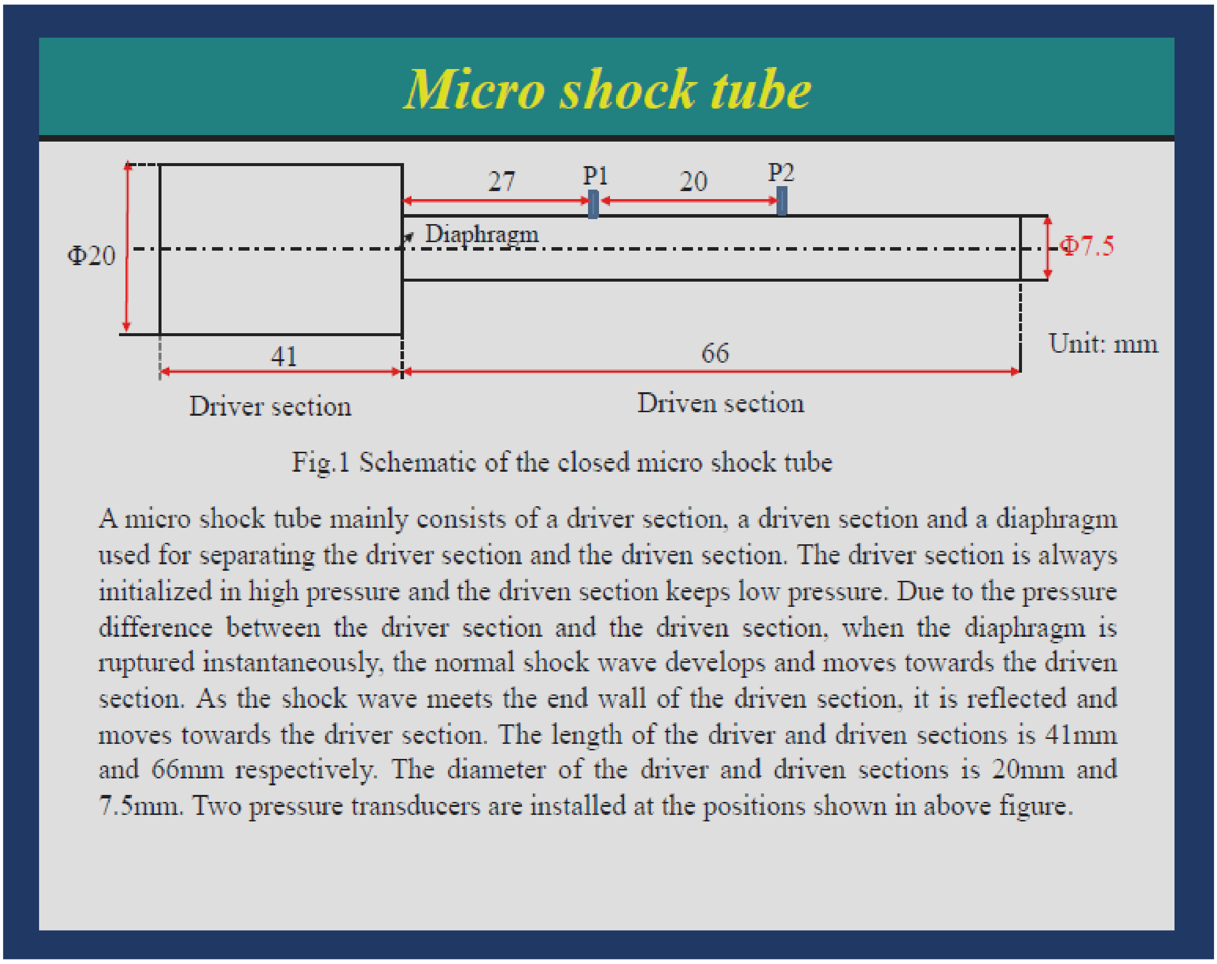

Concentration Heat and Momentum Limited, Bakery House, 40 High Street, Wimbledon, London SW19 5AU, UK
Telephone: 020 8947 7651 Fax: 020 8879 3497
E-mail: rhinocfd@cham.co.uk, Web site: http://www.cham.co.uk

Macro-shock tube

As a precursor to considering the micro shock tube, CHAM undertook a 1D transient analysis of a traditional ***macro*** shock tube for which there is an analytical solution [1]. The purpose of this simulation was both validation and to demonstrate the ability of PHOENICS to capture the moving shock wave, contact discontinuity and rarefaction wave. These phenomena are also present in the ***micro*** shock tube but, as mentioned earlier, under the influence of significant viscous effects and at high-Knudsen numbers, rarefaction effects also come into play.

The tube length and time period are chosen such that the computation ends before the two waves reflect from the ends of the tube. The simulation employs a uniform mesh of 100 cells to cover a 10m long tube with a cross-sectional area of 0.1m2. The transient simulation is run for a time period of 6.1 msec using 100 uniform time steps. The initial conditions are zero velocity with the following settings in each chamber: *Driver Gas*; pressure = 1.0 bar, temperature = 348.391 K and density = 1.0 kg/m3; *Driven Gas*; pressure = 0.1 bar, temperature = 278.13 K and density = 0.125 kg/m3. Wall friction is ignored and the energy equation is solved in terms of static enthalpy with an ideal-gas equation of state. The second-order Van Leer MUSCL scheme is used for the discretisation of convection, and the default first-order Euler scheme is used for the transient terms.
CFD simulations were also made using the OpenFOAM® CFD solver set up via CHAM's recently released **"PH2OF"** (PHOENICS to OpenFOAM) user interface. Both codes used the same computational grid, time step and spatial convection schemes.

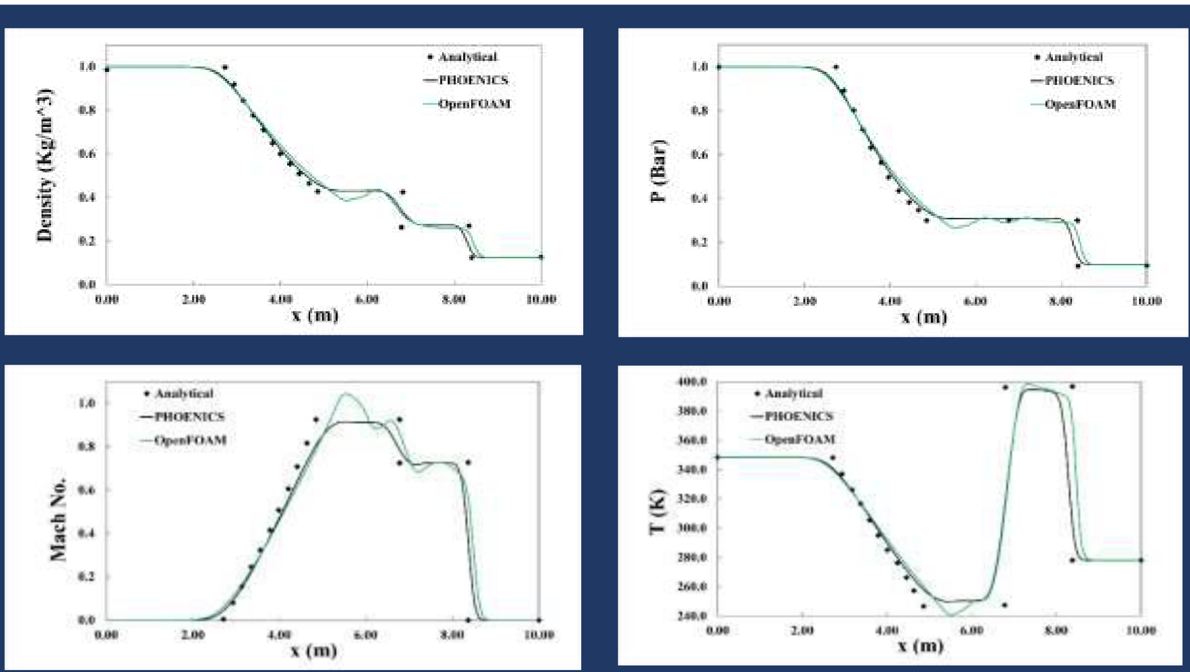

Figure2 Macro shock-tube: PHOENICS, OpenFoam and analytical profiles at t=6.31ms.

Although time constraints precluded experimentation with the various numerical parameters that can influence the accuracy of the solutions, the comparisons made in Fig. 2 show good agreement between OpenFOAM, PHOENICS and the analytical solution. The van-Leer MUSCL scheme was used in these simulations because the default hybrid scheme can produce inferior results due to numerical smearing. It is evident from Fig. 2 that OpenFOAM produces non-physical undershoots and overshoots in the predicted profiles.

Micro-shock tube:

In traditional shock tubes, the shock wave and the contact surface propagate essentially at a constant speed through the tube but, in micro shock tubes, a much thicker boundary layer develops behind the shock wave, which causes the contact surface to accelerate, the shock wave to decelerate, and the flow between these two waves to be non-uniform. For the micro shock tube shown in Fig.1, the initial conditions are zero velocity at a temperature of 300K with Driver and Driven chamber pressures of 9.0 and 1.0 atmospheres respectively. In this case, the pressure of the driven gas is high enough for rarefaction effects to be absent. This situation has been investigated experimentally by Andong University, who performed static-pressure measurements over a time period of 550µsec, as shown in Fig. 3. These measurements were made at sensor points S1 and S2, which are synonymous with the locations P1 and P2 shown in Fig.1. Fig. 3 also includes CFD results obtained by Andong University using Fluent®.

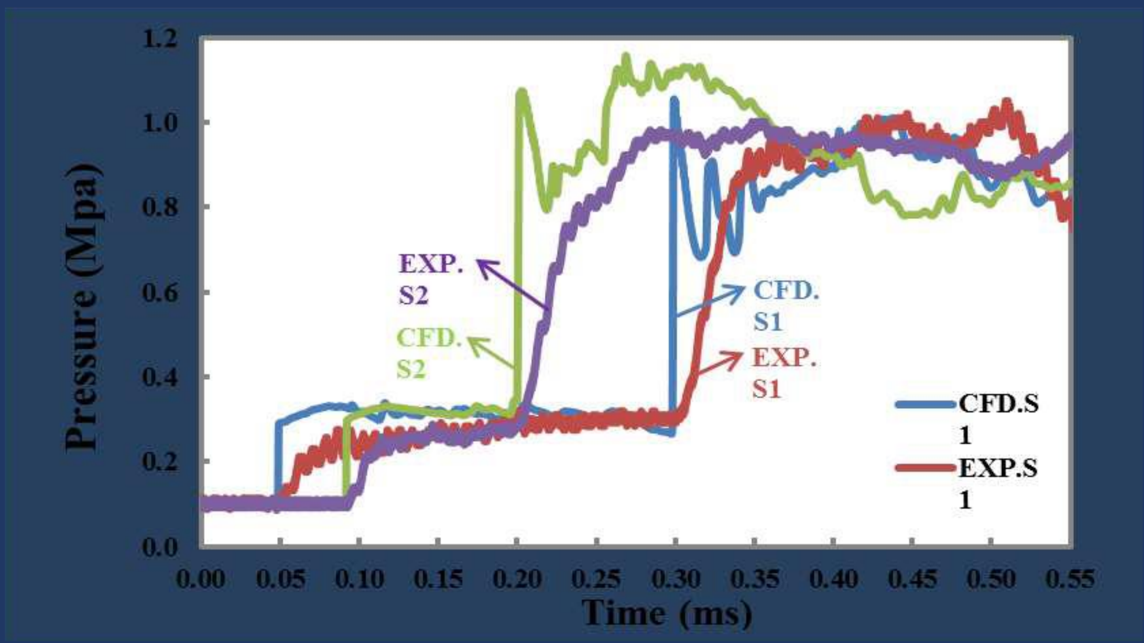

Figure 3 Micro shock-tube: Measured and predicted pressure histories at sensors P1 and P2.

Transient, 2d axisymmetric simulations were made with all three codes using the structured, cylindrical-polar mesh specified by Andong University. This grid employs 160 radial by 1900 axial cells, of which 80 radial by 1172 axial are located in the driven section, and 160 radial by 728 axial cells in the driver section. Each simulation was run for a time period of 500µsec using the uniform time steps in Table 1. With OpenFOAM, convergence difficulties were encountered when using time steps larger than 0.1μs. It is partly for this reason that PHOENICS ran 20% faster than OpenFOAM.

Table 1 also lists the main computational details, including the energy formulation and low- Reynolds-number turbulence model used by each CFD code. An additional run was made using OpenFOAM with the Jones-Launder low-Reynolds-number k-ε model, but this made very little difference to the results.

For all simulations, Sutherland's law was used for the molecular viscosity together with a uniform specific heat of 1004 J/kgK, and laminar and turbulent Prandtl numbers of 0.71 and 0.86 respectively in the energy equation. The PHOENICS & OpenFoam simulations were run in sequential mode on a 3.4GHz Intel Core i7 CPU with 16GB RAM. The Fluent simulations were run by Andong University in Parallel mode on 16 processors, which seems a lot of processors for the specified mesh of 0.21 million active cells. Presumably the significantly longer computer time taken by FLUENT is due the use of the much smaller time step of 0.01 μs.

	PHOENICS	**OpenFOAM**	**Ansys Fluent**
Energy Equation	Static enthalpy (h)	Internal energy (e)	Internal energy (e)
Time Step	0.5ℵσ	0.1ℵσ	0.1ℵσ
Velocity Arrangement	Staggered	Co-located	Co-located
Turbulence Model	2- layer k-ℵ	k-ℵSST	k-ℵSST
Solution algorithm	Implicit SIMPLEST	Implicit PIMPLE (PISO/SIMPLE hybrid)	Explicit? Density-based Coupled Solver with AUSM Flux Splitting
Time differencing scheme	1st Order Euler	1st Order Euler	2nd Order?
Convection discretisation scheme	2nd Order MUSCL	2nd Order MUSCL	2nd Order Linear Upwind?
Elapsed runtime (0.5ms)	22.3 hours	28.03 hours	72 hours

Table 1: Micro Shock Tube: Main Computational Details

Fig. 4 below compares the contour plots of density, temperature, pressure and absolute velocity produced by PHOENICS and OpenFOAM some 0.1msec after rupture of the diaphragm. The plots show the normal shock wave moving to the right through the driven section, and the expansion wave propagating to the left through the driver section. It can be seen that the shock wave gives the driven gas a severe acceleration accompanied by a jump of temperature, pressure and density. It is not shown here, but the predictions also show the expected further increase of temperature, pressure and density of the driven gas when the shock wave is reflected back from the closed end wall. Fig. 4 also reveals that OpenFOAM predicts sharper rarefaction waves expanding into the driver section, as well as sharper waves and reflections just downstream of the diameter reduction in the driven section. The crisper wave capture of OpenFOAM is probably due the much smaller turbulent viscosities produced by the k-▯ SST model. Specifically, the 2-layer k-▯ model introduces a smearing effect by producing excessive turbulent viscosities across shock waves and contact discontinuities. It would be a fairly straightforward matter to implement the k-▯ SST model into PHOENICS by means of the InForm facility in the Q1 input file. An additional PHOENICS run was made using the Sarkar compressibility corrections [2] to the 2-layer k-▯ model, which are intended to reduce the predicted turbulence levels due to dilatational effects in high-speed compressible flow. However, this modification effected very little change in the solution.

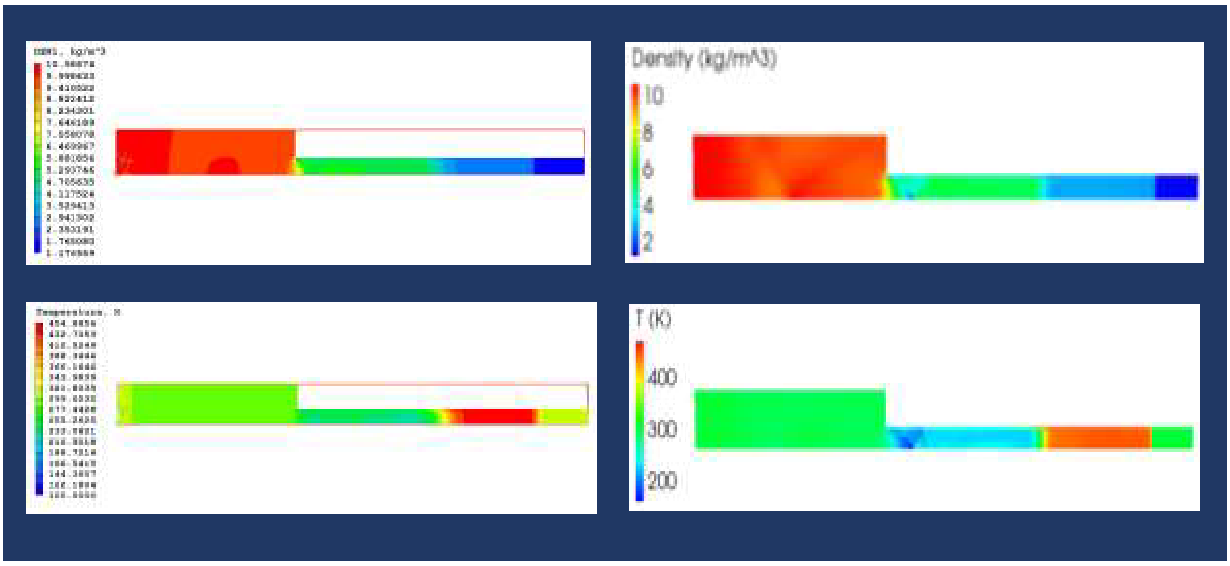

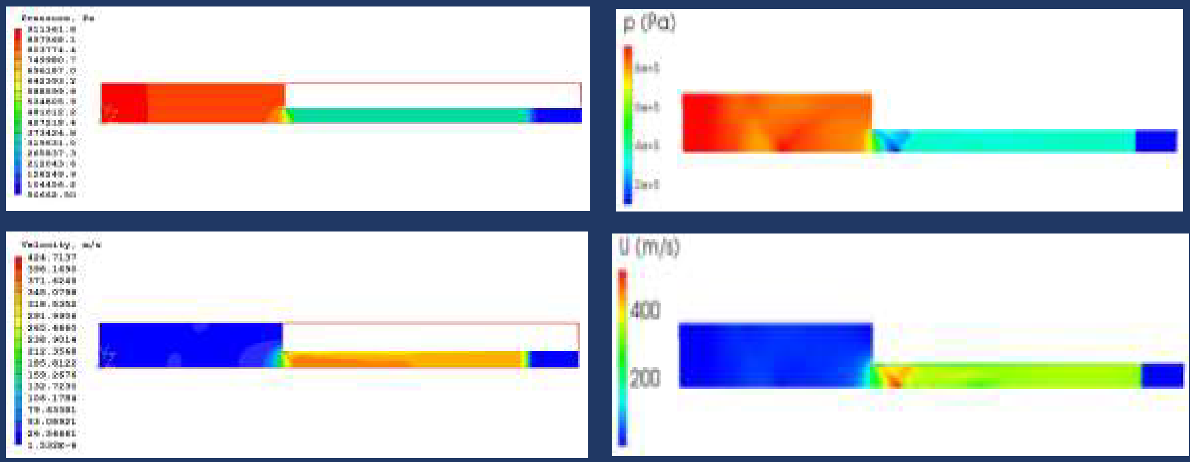

PHOENICS **OpenFOAM**

Fig.4 Micro shock-tube: Contour plots of field variables after 0.1ms.

Figures 5 and 6 compare the measured and predicted pressure histories at the two sensor points located on the outer wall of the driven section. A comparison is made between PHOENICS, OpenFOAM, Fluent and the experimental data. The results produced by all three codes are broadly in line with experiment. PHOENICS and Fluent predict well the shockwave arrival times at S1 and S2 for both the initial and reflected shock wave, respectively. However, OpenFOAM predicts a faster arrival time for the reflected shockwave.

Both OpenFOAM and PHOENICS over-predict the pressure level within the driven section of the shock tube during the latter stages of the simulation. Similar PHOENICS results to those reported here were published in an independent PHOENICS study by Mukhambetiyar et al [3]. It is evident that Fluent was able to predict a better level for the pressure in this period, perhaps due to the much smaller time step combined with second-order time differencing. However, the large fluctuations in pressure predicted by Fluent are not present in the measurements, and they may indicate the presence of non-physical undershoots and overshoots in the solution due to the unbounded nature of the linear-upwind scheme. Such non-physical wiggles were also observed by Lamnaouer [4] in his simulation of macro shock tubes, which he attributed to the absence of a flux limiter in the MUSCL scheme of Fluent.

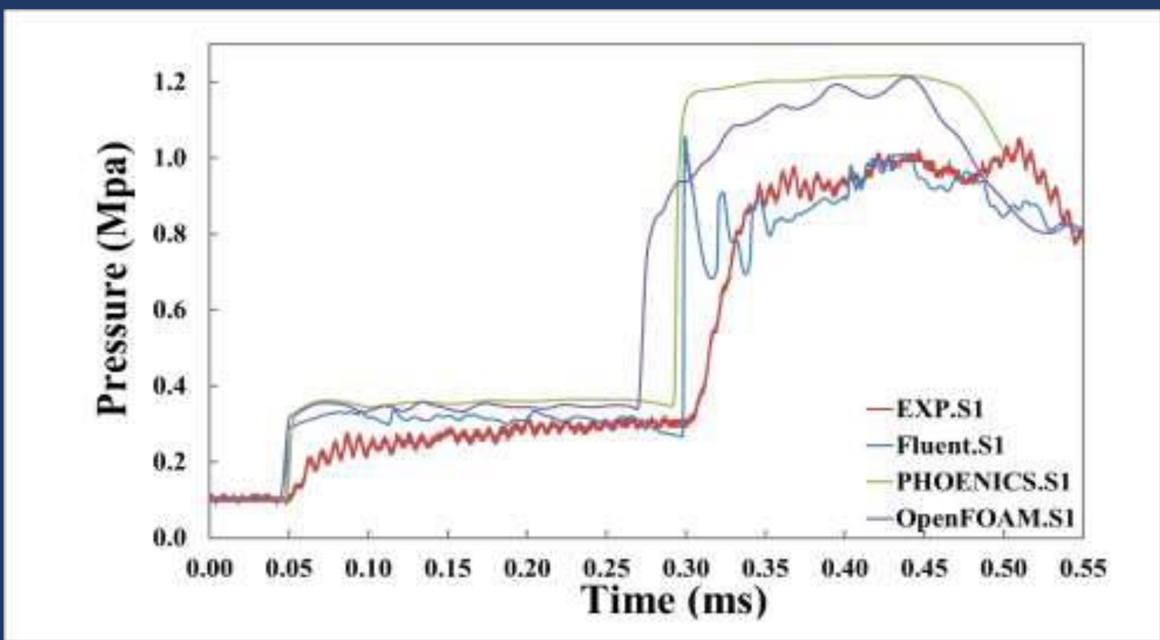

Fig.5 Micro shock-tube: Measured and Predicted pressure histories at the Sensor S1.

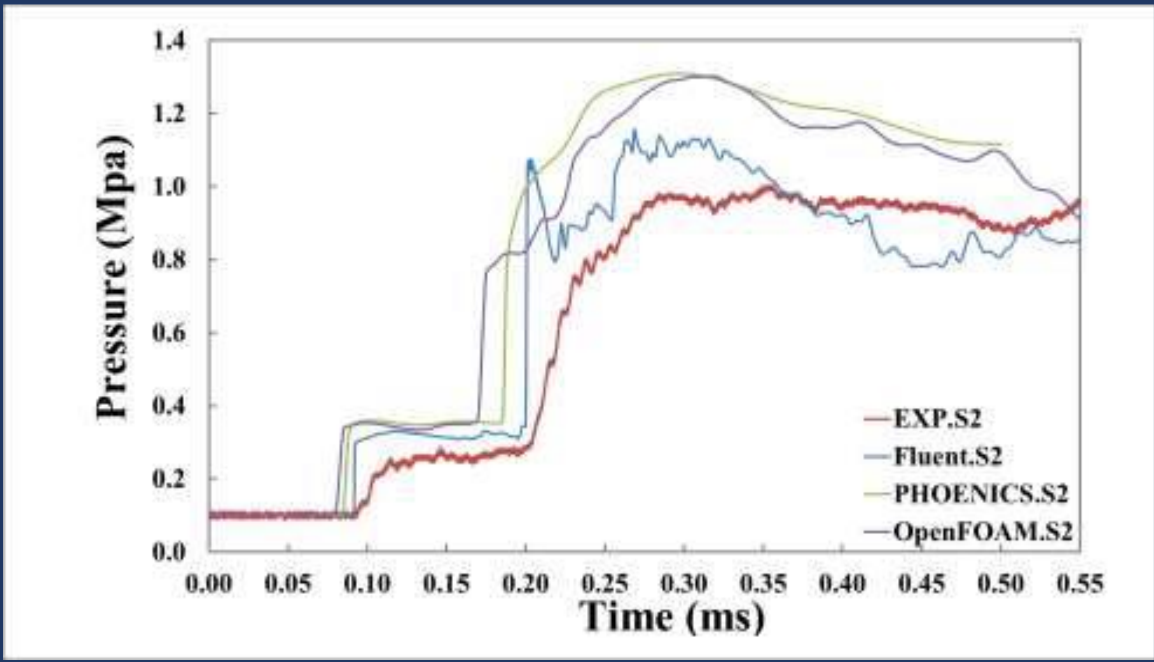

Fig.6 Micro shock-tube: Measured and Predicted pressure histories at the Sensor S2.

Further work is needed to investigate the reasons for the discrepancies between the three codes and experiment. The sensitivity of the PHOENICS solutions to mesh numbers and time-step size needs be explored, and since PHOENICS 2018 is also now equipped with k-ω SST model, it will be a simple matter to repeat the simulations using this less-diffusive turbulence model. The use of a higher-order temporal differencing is another avenue to explore, as well as the use of an alternative higher-order convection discretisation scheme.

References

1. Sod, G. A. (1978), "A survey of several finite difference methods for systems of nonlinear hyperbolic conservation", J. Comp. Physics, Vol. 27, pp. 1-31.
2. Sarkar, S., Erlebacher, G., Hussaini, M. Y., and Kreiss, H. O., (1991), "The analysis and modelling of dilatational terms in compressible turbulence", J. Fluid Mech., Vol. 227, pp473-493.
3. Mukhambetiyar, A, Jaeger, A.M. and Adair, (2017), "CFD modelling of flow characteristics in micro shock tubes", Journal of Applied Fluid Mechanics, Vol. 10, No. 4, pp. 1061-1070.
4. Lamnaouer, M., (2010), "Numerical modelling of the shock tube flow fields before and during Ignition delay time experiments at practical conditions". PhD Thesis, University of Central Florida, Orlando, Florida, USA.